Aerosol and Air Quality Research

Local versus Regional Contributions to PM$_{10}$ Levels in the Western Mediterranean

Álvaro Clemente, Nuria Galindo, Jose F. Nicolás, Javier Crespo, Carlos Pastor, Eduardo Yubero[*]

Atmospheric Pollution Laboratory (LCA), Department of Applied Physics, Miguel Hernández University, Avenida de la Universidad S/N, 03202 Elche, Spain

ABSTRACT

In this study, PM$_{10}$ daily samples were collected every day during approximately one month in winter and one month in summer, 2019. Sampling was performed simultaneously at two different locations: an urban traffic site (∼80 m a.s.l.) and a regional background station (∼1500 m a.s.l.) in the western Mediterranean. The objective of this work was to investigate PM$_{10}$ sources at both sites in order to determine regional and urban contributions to aerosol levels. Seven factors were obtained at both sites using Positive Matrix Factorisation (PMF): *Saharan dust*, *Aged sea salt*, *Ammonium sulfate*, *Nitrate*, *Road traffic*, *Local dust* and *Fresh sea salt*. At the urban site, the contribution of vehicle related sources (*Road traffic*, *Nitrate* and *Local dust*) was significantly higher in winter (∼80%) than in summer (∼60%). The average contribution of *Saharan dust* to PM$_{10}$ levels was much larger at the mountain site (33%) than at the urban location (9%), due to the absence of significant anthropogenic emission sources in the vicinity of the regional background sampling station.

Keywords: PM$_{10}$, PMF, Sources, Regional, Urban, Mountain site

1 INTRODUCTION

The important role of atmospheric aerosols regarding human health (Kim *et al.*, 2015), ecosystems (Grantz *et al.*, 2003), climate change (Zhang *et al.*, 2012), and visibility impairment (Khanna *et al.*, 2018) has led to an increased interest in studying their sources and physicochemical properties. Both natural processes and human activities release airborne particles. The main natural sources of primary particles are wind-blown desert dust, sea spray, and wildfires (EEA, 2012; Viana *et al.*, 2014). Anthropogenic sources include fuel combustion associated with power generation, residential heating and vehicles, tire, brake and road wear from traffic, dust resuspension by traffic, biomass burning and industrial activities (Bonvalot *et al.*, 2019; Groma *et al.*, 2022; Piscitello *et al.*, 2021). There are also secondary aerosols formed from the reaction of gaseous precursors generating low-volatility products, such as sulfuric acid and high-molecular weight organics, that nucleate to form new particles (Dawson *et al.*, 2012; Nault *et al.*, 2021; Zhang *et al.*, 2021). Therefore, aerosols are composed of a variety of inorganic and organic species including primary (elemental carbon, metal oxides, crustal material, sea salt, and fresh organic aerosols) as well as secondary components (ammonium sulfate and nitrate, and oxidized organic compounds).

Source identification and apportionment of aerosols is a helpful tool for the design of mitigation strategies to meet air quality standards. Additionally, the contribution of sources to particulate matter (PM) concentrations has been used in health effect studies in order to identify those sources more strongly linked to health impacts (Daellenbach *et al.*, 2020; Hopke *et al.*, 2020a). Receptor models such as Positive Matrix Factorization (PMF) have been extensively used for aerosol source apportionment at different types of locations (Cesari *et al.*, 2018; Clemente *et al.*, 2021; Galindo *et al.*, 2021; Weber *et al.*, 2019; Wei *et al.*, 2022). These techniques are based on chemometric analysis of the concentrations of aerosol components at the receptor site to identify source-types
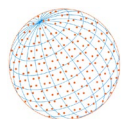
and estimate their contributions to the measured aerosol concentrations (Belis *et al.*, 2013).

According to a recent study, non-urban aerosol sources (i.e., regional/continental sources, both natural and anthropogenic in nature) may account for a significant fraction (> 60%) of PM mass concentrations at urban background sites, preventing many cities from achieving air quality standards only through mitigation measures at the local level (Pandolfi *et al.*, 2020). In fact, these sources are frequently responsible for the exceedances of PM limit values established by the European legislation, particularly in southern European urban areas (Diapouli *et al.*, 2017; Dimitriou *et al.*, 2021; Nicolás *et al.*, 2008). Performing concurrent measurements of PM levels and chemical composition at paired sites, especially at urban and regional background locations, can help distinguishing between local and regional/continental sources (Pandolfi *et al.*, 2020). Many previous works have been focused on PM source apportionment in urban areas (e.g., Alebić-Juretić and Mifka, 2022; Cesari *et al.*, 2018; Jain *et al.*, 2020; Hama *et al.*, 2018; Ramírez *et al.*, 2018), including a study performed at an urban background site in Elche (the same area as this study) (Nicolás *et al.*, 2008). Alternatively, some source apportionment studies have been carried out at regional background and/or remote sites (e.g., Borlaza *et al.*, 2022; Cerro *et al.*, 2020; Marenco *et al.*, 2006; Ripoll *et al.*, 2015). However, few studies combine simultaneous measurements at urban and remote sites (Ealo *et al.*, 2018; Pandolfi *et al.*, 2020; Weber *et al.*, 2019).

The study of aerosols at regional background stations located at high altitude regions can provide information on the background aerosol concentration and chemical composition (i.e., well away from direct local anthropogenic emissions) in a certain geographic area (Deabji *et al.*, 2021; Galindo *et al.*, 2016). Additionally, these sites are very suitable for assessing the influence of long-range transport of air masses on the aerosol load, composition and physical properties (Castañer *et al.*, 2017; Galindo *et al.*, 2017; Ram *et al.*, 2010; Salvador *et al.*, 2010). In the present work, the contributions of sources to PM_{10} (particulate matter with a diameter of 10 µm or less) during one month in winter and one month in summer at two different locations in the western Mediterranean basin were investigated: an urban traffic site (~80 m a.s.l.) and a high-altitude station (~1500 m a.s.l.). Aerosol source apportionment was performed using the PMF model. The main objective of this work is to disentangle local and regional sources of aerosols in southeastern Spain in summer and winter.

2 MATERIALS AND METHODS

2.1 Study Sites
Two air quality stations were monitored in southeastern Spain. The urban traffic site was located in Elche, a medium-sized city (~190,000 inhabitants) approximately 12 km from the closest Mediterranean coast and 86 m a.s.l. (Fig. 1). The climate in this area can be classified as dry Mediterranean and is characterized by soft winters and warm summers (average temperatures of 12°C and 25°C, respectively), along with a low annual rainfall (< 300 mm) and a high number of sunshine hours (> 3000 a year). PM_{10} samples were collected on the first floor (~4.5 meters above ground level) of a municipal office block next to a seven-meter wide street with two traffic lines in the same direction. More information about this sampling site can be found in Galindo *et al.* (2018).

The regional background station was located at Mt. Aitana (1558 m a.s.l.), the highest peak of the Betic mountain range, which is ~56 km northeast from the sampling point in Elche and 16 km from the Mediterranean Sea (Fig. 1). This monitoring site is surrounded by a semi-arid area where soils are sparsely covered by sclerophyllous and xerophilous vegetation such as pines and bushes, and typical Mediterranean crops (e.g., olive and almond trees). The influence of local anthropogenic emissions at this site is negligible due to the absence of big urban agglomerations nearby and the complex orography of the area. The station is most of the time in the free troposphere between November and January, whereas from June to September it is mainly within the planetary boundary layer (Nicolás *et al.*, 2018). A more detailed description of this sampling point can be found in Castañer *et al.* (2017) and Galindo *et al.* (2017).

2.2 Sample Collection and Analysis
Two intensive sampling campaigns were carried out in February and July 2019. During these
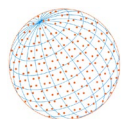
Fig. 1. Location of the urban traffic and regional background sampling sites in the western Mediterranean Basin.

campaigns PM$_{10}$ daily samples were collected every day at both locations simultaneously. A total of 72 valid samples were collected in the city center of Elche (37 in winter and 35 in summer), while 60 valid samples were gathered at Mt. Aitana (27 in winter and 35 in summer). Derenda 3.1 low-volume samplers (2.3 m^3 h^{-1}) were used for sample collection, using Ahlstrom quartz fiber filters as substrates for particle deposition (47 mm diameter).

Filters were weighed using an analytical balance with 10 µg sensitivity (Ohaus, model AP250D) both before and after sampling in order to determine PM$_{10}$ concentrations. Before weighing, filters were kept under stable temperature (20 ± 1°C) and relative humidity (50 ± 5%) conditions for at least 24 hours.

After the gravimetric procedure, the metal content of the PM$_{10}$ samples was determined by Energy Dispersive X-Ray Fluorescence (ED-XRF) with an ARL Quant'x Spectrometer (Thermo Fisher Scientific, UK). In this work, concentrations of selected metals (Ca, Ti, V, Cr, Mn, Fe, Ni, Cu, and Zn) are presented. More details about the analytical procedure can be found in Chiari *et al.* (2018).

After the elemental analysis, 1.5 cm^2 punches from the PM$_{10}$ samples were analyzed by the Thermal-Optical Transmittance method in order to determine organic carbon (OC) and elemental carbon (EC) concentrations. A Thermal-Optical Carbon Aerosol Analyser (Sunset Laboratory, Inc.) with the EUSAAR2 protocol was employed (Cavalli *et al.*, 2010).

Finally, the remaining filter was extracted with 8 mL of ultrapure water in an ultrasonic bath for 45 minutes. The resulting extracts were analyzed by ion chromatography in order to quantify the water-soluble ion concentrations (Cl$^-$, NO$_3^-$, SO$_4^{2-}$, C$_2$O$_4^{2-}$, Na$^+$, NH$_4^+$, K$^+$, Mg^{2+}, and Ca^{2+}). Cations were determined with a Dionex ICS-1100 ion chromatograph equipped with a CS12A separation column (4 × 250 mm) and methane sulfonic acid as eluent (20 mM, 0.8 mL min^{-1}). Anions were analyzed with a Dionex DX-120 ion chromatograph equipped with an AS11-HC analytical column (4 × 250 mm) and NaOH as eluent (15 mM, 1 mL min^{-1}). Carbonate concentrations were estimated from the anion deficit as described in Nicolás *et al.* (2009).

2.3 Positive Matrix Factorization

The Positive Matrix Factorization (PMF) technique was developed by Paatero and Tapper (1994). This method solves the mass balance equation (Eq. (1)) with a weighted least squares approach.
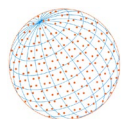
$$x_{ij} = \sum_{k=1}^{p} g_{ik} f_{kj} + e_{ij} \tag{1}$$

where x_{ij} is the concentration of the jth species in the ith sample, p is the number of factors, g_{ik} is the mass contribution of the kth factor to the ith sample, f_{kj} represents the concentration of the jth species in the kth factor profile and e_{ij} is the difference between modelled and measured concentrations (x_{ij}).

When using this type of models, it must be kept in mind that factors can represent a single source or source category (e.g., traffic, wood burning), a chemical compound (e.g., ammonium nitrate), or mixtures of sources and compositions (Hopke *et al.*, 2020b).

PMF solves Eq. (1) by applying non-negative constraints to factor contributions (g_{ik}) and to species concentrations in source profiles (f_{kj}) while trying to minimize the object function in Eq. (2) (Belis *et al.*, 2013).

$$Q = \sum_{i=1}^{n} \sum_{j=1}^{m} \left(\frac{x_{ij} - \sum_{k=1}^{p} g_{ik} f_{kj}}{u_{ij}} \right)^2 \rightarrow Q = \sum_{i=1}^{n} \sum_{j=1}^{m} \left(\frac{e_{ij}}{u_{ij}} \right)^2 \tag{2}$$

where n is the number of samples, m is the number of measured chemical species and u_{ij} is the uncertainty associated with the concentration value x_{ij}.

The U.S. EPA PMF 5.0 version was employed in this study to carry out the source apportionment at the urban traffic and mountain sites. In order to get more reliable results with the PMF model, non-simultaneous samples collected outside the study period at both sites during 2019 were added to those simultaneously collected during the study period (February and July 2019), to reach a total of 100 samples for each site. It was assumed that such profiles do not change significantly over time (Belis *et al.*, 2013).

Twenty-two chemical species were included in the input matrix for each site and were classified as *Strong*, *Weak* and *Bad* according to their signal-to-noise ratio (S/N) (Paatero and Hopke, 2003) and the percentage of values above the detection limit. For both locations, Ca^{2+} was discarded from the source apportionment to avoid double mass counting.

Preliminary runs for each site separately showed that both locations were influenced by a similar set of factors. Nevertheless, in some cases (e.g., road traffic) the same factor had significantly different chemical profiles at both sites. In this regard, EC at Mt. Aitana was classified as *Bad* due to the low percentage of samples above the detection limit and its low S/N ratio, while at the urban site all samples had EC concentrations above the detection limit and the S/N ratio was > 2.

3 RESULTS AND DISCUSSION

3.1 Chemical Composition and Seasonal Variation

Tables 1 and 2 summarise the main statistics for PM_{10} data at both sampling sites during the whole study period. The average PM_{10} concentration at the Aitana mountain site (14.3 ± 9.9 μg m^{-3}) was less than half that found in Elche (32.9 ± 11.7 μg m^{-3}) in the same period. A similar average PM_{10} concentration was registered at the Aitana station in a sampling campaign carried out between March 2014 and September 2015 (13.3 ± 12.1 μg m^{-3}; Galindo *et al.*, 2017). These values were of the same order than those recently reported for a remote site in northern France (13.0 μg m^{-3}; Weber *et al.*, 2019), but significantly lower than the concentration measured at a high-mountain site (29.2 ± 17.3 μg m^{-3}) located in the Middle Atlas Mountains (2100 m a.s.l.; Deabji *et al.*, 2021). This can be attributed to the high contribution of mineral dust (17.7 ± 7.4 μg m^{-3}) due to the close proximity of this station to the Sahara Desert (~300 km).

At the urban site the average PM_{10} concentration was not very different from that obtained in previous studies (27 μg m^{-3}; Galindo *et al.*, 2019). However, both values are not fully comparable since the number of samples in the present study was considerably lower and the averaging period
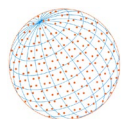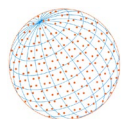
Table 1. Summary of the concentrations of PM_{10} and chemical species at Mt. Aitana. Averages, standard deviations (SD), minimum and maximum values and percentage of values above the detection limit (ADL) are included. The percentage contribution of each species to the average PM_{10} concentration is also shown.

	Average	SD	Min	Max	ADL (%)	% of PM mass
PM_{10} ($\mu g\ m^{-3}$)	14.3	9.9	1.2	48.5	—	—
OC	2.95	0.58	1.68	3.97	100	21
EC	0.05	0.06	< mdl	0.17	45	0.3
Cl^-	0.04	0.05	< mdl	0.24	85	0.3
NO_3^-	0.75	0.45	0.16	2.02	100	5
SO_4^{2-}	1.46	0.91	0.19	3.63	100	10
$C_2O_4^{2-}$	0.19	0.11	0.02	0.38	100	1
CO_3^{2-}	0.41	0.29	< mdl	1.61	95	3
Na^+	0.23	0.18	< mdl	0.91	89	2
NH_4^+	0.21	0.18	< mdl	0.68	87	1
K^+	0.07	0.04	< mdl	0.21	80	0.5
Mg^{2+}	0.05	0.03	0.01	0.14	100	0.4
Ca (ng m^{-3})	590	429	13	2290	100	4
Ti	30	35	< mdl	153	80	0.2
V	5	6	< mdl	27	48	0.04
Cr	6	3	< mdl	12	92	0.05
Mn	12	10	< mdl	50	98	0.1
Fe	292	295	34	1331	100	2
Ni	18	4	12	31	100	0.1
Cu	5	1	2	7	100	0.03
Zn	16	3	9	22	100	0.1

Table 2. Summary of the concentrations of PM_{10} and chemical species at the Elche city center. Averages, standard deviations (SD), minimum and maximum values and percentage of values above the detection limit (ADL) are included. The percentage contribution of each species to the average PM_{10} concentration is also shown.

	Average	SD	Min	Max	ADL (%)	% of PM mass
PM_{10} ($\mu g\ m^{-3}$)	32.9	11.7	5.3	66.4	—	—
OC	6.52	1.87	2.65	11.00	100	21
EC	0.84	0.30	0.17	1.60	100	3
Cl^-	0.62	0.60	0.09	3.23	100	2
NO_3^-	3.12	1.91	0.16	10.50	100	9
SO_4^{2-}	3.30	1.83	0.24	9.15	100	10
$C_2O_4^{2-}$	0.26	0.09	0.04	0.44	100	1
CO_3^{2-}	1.67	1.14	< mdl	4.27	88	5
Na^+	0.86	0.60	< mdl	2.80	99	3
NH_4^+	0.56	0.42	< mdl	1.93	97	2
K^+	0.24	0.14	0.07	0.70	100	1
Mg^{2+}	0.17	0.08	0.06	0.44	100	1
Ca (ng m^{-3})	1943	958	434	5518	100	6
Ti	26	19	5	119	100	0.1
V	9	6	< mdl	33	75	0.03
Cr	11	3	8	20	100	0.03
Mn	18	7	8	45	100	0.1
Fe	501	216	144	1520	100	1.5
Ni	23	4	15	38	100	0.1
Cu	18	6	8	33	100	0.1
Zn	35	10	18	83	100	0.1

was different. Additionally, interannual variations in PM concentrations may occur depending on the meteorological conditions and the frequency of PM events (Galindo *et al.*, 2020; Ji *et al.*, 2020). The mean concentration obtained in Elche was similar to those registered at other low industrialized cities within the Mediterranean basin (Cesari *et al.*, 2018; Dimitriou and Kassomenos, 2017). Compared with the values found at other urban areas in Spain, the average concentration measured in the present study was higher than that found at an urban background site in Gijón (19.1 µg m^{-3}; Megido *et al.*, 2016). On the other hand, the average winter PM$_{10}$ concentration in Elche (34.1 µg m^{-3}; Table 3) was higher than the value registered in Barcelona (12.5 µg m^{-3}—winter average, van Drooge *et al.*, 2022) and of the same order than that reported for Granada, a middle-large city located in the southeast of Spain (28.5 µg m^{-3}-winter average, van Drooge *et al.*, 2022).

The chemical species that contributed the most to the PM$_{10}$ mass were the same at both locations: OC (~21%), secondary inorganic species (21% and 17% in Elche and Aitana, respectively), calcium (6% and 4%, respectively) and carbonate (5% and 3%, respectively). At Mt. Aitana sulfate was the major constituent of the inorganic salts, accounting for 63% of the secondary inorganic species and 10% of the total PM$_{10}$ mass concentration. It has been found that organic carbon and sulfate are the major aerosol constituents at other high mountain sites like Mt. Cimone, Italy (Cristofanelli *et al.*, 2018), and the Nepal Climate Observatory-Pyramid, in the Himalayan mountain range (Decesari *et al.*, 2010). The chemical composition of PM$_{10}$ at urban sites is highly variable depending on the sources and meteorological conditions of the study area. Thus, OC has been identified as the main chemical component of the PM$_{10}$ fraction in previous studies performed at urban locations, contributing between approximately 20 and 30% (Cesari *et al.*, 2018; Furman *et al.*, 2021; Ramírez *et al.*, 2018), while other works have reported a clear dominance of secondary inorganic species (Hama *et al.*, 2018; Jain *et al.*, 2020).

In terms of atmospheric concentration (µg m^{-3}), all the analyzed species, except titanium, showed higher levels in Elche than in Aitana. Most of them were two to four times higher at the urban site. EC and Cl$^-$ average concentrations in Elche were 20 and 15 times higher, respectively, than in Aitana. In fact, EC levels were below the detection limit in more than 50% of the samples collected at the high-mountain station. While EC is considered a tracer of traffic exhaust emissions (Keuken *et al.*, 2013; Megido *et al.*, 2016), chloride is mostly associated with marine aerosols. The closer proximity of the urban site to the coast may explain the higher levels of Cl$^-$ and the other marine ions (Na$^+$ and Mg^{2+}) with respect to those measured at the Aitana station. The fact that the ratio between chloride concentrations measured at the urban and regional background sites (~15) was considerably higher than those calculated for sodium and magnesium (~4) could be attributed to the loss of chloride by reactions of NaCl with acidic species during the transport of marine aerosols inland. The average concentration of NO$_3^-$ in Elche was four times higher than in Aitana. Atmospheric nitrate's main formation pathway is the oxidation of traffic derived NO$_x$. As expected, elements such as Cu, Zn, and Fe, which are emitted from brake and tire abrasion (Piscitello *et al.*, 2021), also showed higher concentrations in Elche. Most of the crustal elements (e.g., Ca and Fe; Piscitello *et al.*, 2021) were more abundant at the urban site, although they are also present in Saharan dust that often affects the Aitana sampling site (Galindo *et al.*, 2017). Thus, the notable increment of these species at the urban station highlights the importance of non-exhaust emissions from road traffic as a contributor to PM$_{10}$ levels.

Regarding Ti, its average mass concentration was slightly higher at the Aitana station than at the Elche sampling site, although the difference was not statistically significant. Titanium is considered as a reliable tracer for Saharan dust in the study area (Galindo *et al.*, 2017, 2018). High mountain stations are very sensitive to this type of event, since the influence of local anthropogenic sources is scarce (Cristofanelli *et al.*, 2018; Galindo *et al.*, 2017; Moroni *et al.*, 2015).

Average concentrations of PM$_{10}$ and chemical species in the winter and summer campaigns are presented in Table 3. EC seasonal concentrations at Mt. Aitana are not shown because of the high percentage of samples under the detection limit.

At the Aitana station the average PM$_{10}$ concentration in winter (8.5 ± 5.2 µg m^{-3}) was approximately half of that registered in summer (17.4 ± 9.2 µg m^{-3}), as previously observed for both PM$_1$ and PM$_{10}$ (Galindo *et al.*, 2016; Castañer *et al.*, 2017). This can be explained by the decrease in the height of the planetary boundary layer (PBL) during the cold months, which often leaves the top
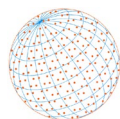
Table 3. Winter and summer average concentrations (± standard deviations) of PM_{10} and chemical species at the regional background and urban sites. The results of the Mann-Whitney U Test used to compare winter and summer values are also shown. Ca^{2+} concentrations are not presented here to avoid double counting with Ca, since at the study area calcium is mainly in the form of soluble salts (Galindo *et al.,* 2020).

	Mt. Aitana			Elche		
	February	July	M-W test	February	July	M-W test
PM_{10} (µg m^{-3})	8.5 ± 5.2	17.4 ± 9.2	*	34.1 ± 11.9	31.7 ± 9.1	
OC	2.64 ± 0.59	3.43 ± 1.29	*	7.37 ± 2.20	5.61 ± 0.75	*
EC				0.99 ± 0.34	0.69 ± 0.15	*
Cl^-	0.06 ± 0.11	0.03 ± 0.04		0.72 ± 0.72	0.51 ± 0.43	
NO_3^-	0.85 ± 0.48	0.63 ± 0.39		3.85 ± 2.03	2.34 ± 1.44	*
SO_4^{2-}	0.62 ± 0.38	1.99 ± 0.66	*	2.42 ± 1.17	4.24 ± 1.95	*
$C_2O_4^{2-}$	0.09 ± 0.04	0.26 ± 0.08	*	0.22 ± 0.09	0.30 ± 0.07	*
CO_3^{2-}	0.31 ± 0.25	0.45 ± 0.23	*	1.57 ± 1.26	1.78 ± 1.00	
Na^+	0.14 ± 0.12	0.31 ± 0.18	*	0.70 ± 0.46	1.04 ± 0.69	*
NH_4^+	0.12 ± 0.13	0.28 ± 0.18	*	0.49 ± 0.46	0.64 ± 0.37	
K^+	0.07 ± 0.04	0.05 ± 0.03		0.32 ± 0.15	0.16 ± 0.05	*
Mg^{2+}	0.03 ± 0.02	0.07 ± 0.02	*	0.15 ± 0.06	0.18 ± 0.09	
Ca (ng m^{-3})	424 ± 289	654 ± 393	*	1935 ± 1083	1951 ± 820	
Ti	13 ± 17	38 ± 38	*	23 ± 17	29 ± 20	
V	2 ± 3	7 ± 7	*	8 ± 5	9 ± 7	
Cr	6 ± 2	7 ± 3	*	11 ± 3	11 ± 2	
Mn	8 ± 5	15 ± 11	*	18 ± 7	18 ± 6	
Fe	158 ± 144	359 ± 320	*	542 ± 248	458 ± 169	*
Ni	16 ± 2	19 ± 4	*	23 ± 4	23 ± 4	
Cu	5 ± 1	5 ± 1		21 ± 7	15 ± 3	*
Zn	16 ± 5	16 ± 3		38 ± 12	31 ± 5	*

* The difference between winter and summer values was statistically significant ($p < 0.05$).

of Mt. Aitana under free troposphere (FT) conditions (Cristofanelli *et al.,* 2018; Tsamalis *et al.,* 2014). This translates into a much lower influence of pollution sources at this monitoring site in winter and allows to explain the higher levels of the majority of PM_{10} components in July.

In the city center of Elche, the average winter PM_{10} concentration (34.1 ± 11.9 µg m^{-3}) was slightly higher than that of summer (31.7 ± 9.1 µg m^{-3}), although this difference was not statistically significant. Moderate differences between winter and summer average PM_{10} concentrations have been observed in earlier campaigns performed at the same site (Galindo and Yubero 2017; Galindo *et al.,* 2020) since they depend on the frequency and intensity of PM events and the predominant meteorological conditions. However, most of the major and trace PM_{10} components showed well-defined seasonal cycles, as discussed in detail in previous studies. Briefly, the concentrations of metals associated with traffic particle emissions (Cu and Zn), as well as those of carbonaceous species and soluble potassium (derived from traffic exhaust, biomass burning, and soils), were higher in winter than in summer due to an increase in emission rates from sources and/or the lower dispersion conditions in wintertime (Galindo *et al.,* 2018, 2019). In contrast sea-salt cations (Na^+ and Mg^{2+}) and secondary inorganic species, namely sulfate and oxalate, exhibited higher average concentrations in summer. This can be explained, respectively, by the prevalence of sea breezes and the increase in the photochemical oxidation of SO_2 and volatile organic compounds during the summer season (Galindo and Yubero 2017). In the case of nitrate and elements commonly associated with road dust, such as Ca and Fe, the seasonal patterns are not as clear and may change depending on the sampling period, as reported in previous works carried out in the study region (Galindo and Yubero 2017; Galindo *et al.,* 2020; Navarro-Selma *et al.,* 2022). The most likely reason, as commented for PM_{10}, is that the concentrations of these components are more affected by specific pollution episodes (such as winter stagnation events and Saharan dust outbreaks) and local meteorological conditions, which show significant year-to-year variations.
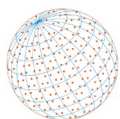
3.2 Positive Matrix Factorization

A seven-factor solution was found to be the most physically applicable solution for the input data at both sites (Fig. 2). For both locations, there was a good correlation between measured and modelled PM_{10} concentrations (Fig. 3).

In order to find the most robust and meaningful solution, different analyses were carried out assuming a different number of final factors. At the Aitana site, the six-factor solution returned two marine factors (*Fresh sea salt* and *Aged sea salt*). However, the *Fresh sea salt* factor showed high levels of nitrate (43% of the total NO_3^- mass), which does not match the expected composition of this source. Hence, this solution was discarded. In the seven-factor solution, nitrate was mainly present in the *Aged sea salt* factor and in a factor named *Nitrate*, related to secondary nitrate particles (e.g., $Ca(NO_3)_2$). Finally, in the eight-source solution, the *Aged sea salt* factor was separated into two correlated factors (as confirmed with the G-space plots), and therefore the previous solution with seven factors was selected as the final solution.

In Elche, trials with the six-factor solution showed low stability of the Q-value and did not allow to distinguish between the fresh sea spray and the aged marine aerosol. In addition, the *Saharan dust* factor seemed to be mixed with the marine factors. The addition of a seventh factor increased the stability of the Q-value and allowed to obtain an independent *Aged sea salt* factor. In the eight-factor solution, the *Saharan dust* factor was separated into two factors without a clear interpretation. The solution with 7 factors was chosen as the one that best explained the sources of aerosols in the city.

The Bootstrap analysis for both sites showed that all factors were mapped between 95% and 100%, except for *Nitrate* (88% of the runs) at the Aitana station. The DISP analysis was valid and no drop of the Q-value was observed.

The seven factors identified at both sites were (factor profiles and temporal variations are shown in the Supplementary Material):

a) *Road traffic + Biomass burning*: this factor includes tailpipe emissions and abrasion processes of vehicle components. It contributed on average 31% to the total PM_{10} concentration in Elche
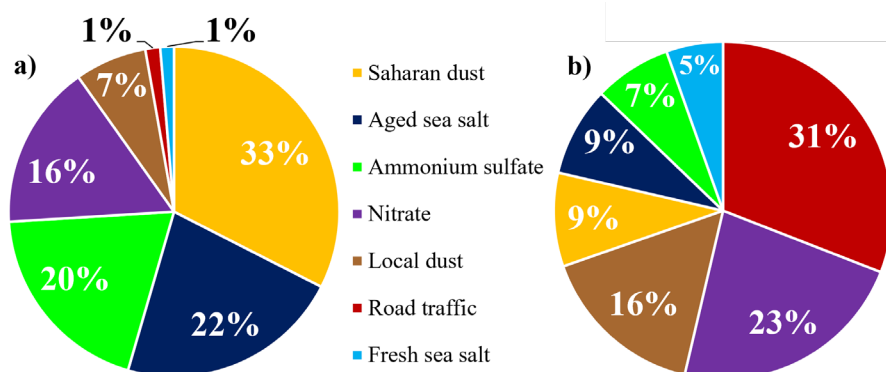

Fig. 2. Average percentage contributions to PM_{10} of the PMF factors at the (a) regional background station and (b) the urban traffic site.
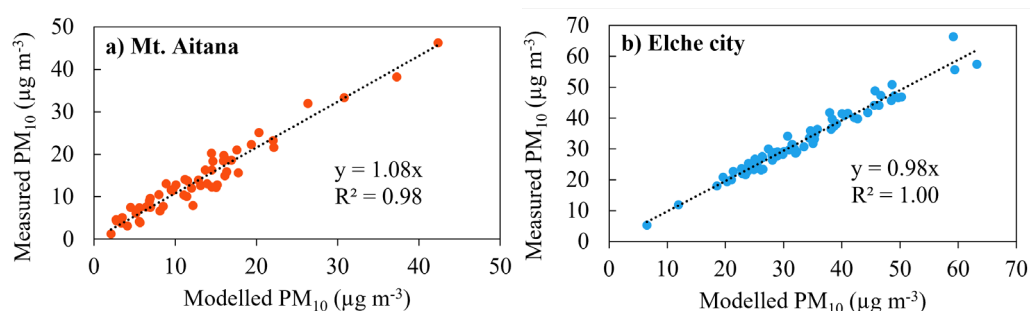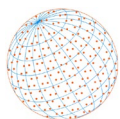

Fig. 3. Scatter plots of measured PM_{10} vs. modelled PM_{10} concentrations at each location.

(10.4 μg m^{-3}) and 1% in Aitana (0.2 μg m^{-3}). The contribution from this source was negligible at the mountain site. However, this factor was still present in solutions with a lower number of factors and always mapped by the Bootstrap analysis. Therefore, it was concluded that there was a marginal influence of anthropogenic sources at the mountain site. This factor explained a large fraction of species usually related to vehicle exhaust such as OC (70% of its total concentration in Elche and 60% in Aitana) and EC (82% in Elche), components associated with brake wear, namely Cu (87% and 76% in Elche and Aitana, respectively) and Cr (57% and 54%, respectively) and Zn (87% and 67%, respectively), a tracer of tire abrasion (Harrison *et al.*, 2021). Also, a high share of K$^+$, which can be derived from traffic exhaust emissions (Wang *et al.*, 2014), was explained by this factor (76% and 49%, respectively, in Elche and Aitana).

The significant presence of soluble potassium may indicate that this factor also includes biomass burning emissions (Samek *et al.*, 2021). Given that traffic and biomass burning share common tracers (OC and EC) and that a specific marker of biomass burning (e.g., levoglucosan) was not quantified, these sources could not be separated from each other. The average contribution of biomass burning to the PM$_{10}$ concentration measured at a residential area close to the city of Elche during winter and spring was estimated to be 8% (Galindo *et al.*, 2021). A lower contribution could be expected at the urban traffic site since it is far from wood combustion emissions.

b) *Nitrate*: the second factor, dominated by NO$_3^-$, was identified at both sampling sites, although it showed slightly different chemical profiles. The average relative contribution of the *Nitrate* factor to the PM$_{10}$ mass concentration was 23% in Elche and 16% in Aitana. The average mass concentration of this factor was significantly higher at the urban site (7.6 μg m^{-3}) than at the regional background station (2.0 μg m^{-3}), which can be explained by the huge difference in road traffic intensities between both sites, as already commented.

At the regional background site, this factor contributed 67% to NO$_3^-$, 45% to K$^+$ and 28% to OC. Although only 15% of the total Ca mass was associated with the *Nitrate* factor, this element was one of the most abundant species in its profile, just below OC and NO$_3^-$ (Fig. S1(d)). Therefore, this factor was linked to the formation or transport of coarse Ca(NO$_3$)$_2$. Due to the lack of ammonia and the thermal instability of ammonium nitrate, the available nitric acid reacts with calcium carbonate to form calcium nitrate.
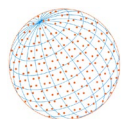
In Elche, this factor contributed 71% to the average nitrate concentration. The second most abundant species in its profile was calcium, although this source only accounted for 12% of the total Ca concentration. Another difference is that this factor contributed 13% to the average NH$_4^+$ concentration measured in Elche. Consequently, at the urban site this factor also included secondary ammonium nitrate.

c) *Local dust*: the average relative contribution of this factor to PM$_{10}$ in the urban area (16%) was statistically higher than at the mountain site (7%). Nevertheless, in terms of mass concentrations this difference was even greater, since PM$_{10}$ levels were six times higher in Elche (5.4 μg m^{-3}) than in Aitana (0.9 μg m^{-3}).

This factor is associated with local dust resuspension, either by natural (e.g., wind) or anthropogenic processes (e.g., road traffic). It is important to mention that local soils are highly enriched in calcium carbonate since the bedrock in this region is primarily calcite (Galindo *et al.*, 2018).

The chemical composition of this source was dominated by CO$_3^{2-}$ (this factor explains 93% of CO$_3^{2-}$ in Elche and 60% in Aitana) and Ca (53% and 47%, respectively, in Elche and Aitana). In addition, the CO$_3^{2-}$/Ca ratio for this factor at both locations (0.7 in Elche and 0.8 in Aitana) is consistent with the stoichiometric ratio of CaCO$_3$ (i.e., 0.7 by mass). Other crustal elements, such as Ti, Mn and Fe, are also present in the profile of this source, especially in Elche, but at much lower percentages.

d) *Saharan dust*: the second dust-related factor is associated with episodes of long-range transport of mineral dust from North Africa. The average mass concentration of this factor was statistically higher at the mountain site than at the traffic station (4.0 μg m^{-3} in Aitana and 3.0 μg m^{-3} in Elche), most likely due to the high altitude transport of desert dust (Baumann-Stanzer *et al.*, 2019; Valenzuela *et al.*, 2015).The relative contribution of Saharan dust to PM$_{10}$ levels was much larger at the mountain site due to the absence of significant anthropogenic emission sources in nearby areas, while at the urban location it fell down to fourth place along with the *Aged sea salt* factor (Fig. 2).

This factor explained the highest fraction of Ti (41% in Elche and 74% in Aitana). At the mountain site, Fe (61%), V (56%) and Mn (51%) were also abundant in the profile. Other species such as Ca (26%), CO_3^{2-} (19%), and SO_4^{2-} (8%) also contributed to this factor (Fig. S1(a)). Although V and Ni are considered tracers of the combustion of residual fuels such as fuel-oil (Corbin *et al.*, 2018; Priyan *et al.*, 2022), significant increases in their concentrations during Saharan dust outbreaks have been previously reported (Galindo *et al.*, 2017, 2018; Millán-Martínez *et al.*, 2021). This has been attributed to the mixing of desert dust with anthropogenic pollutants emitted in North Africa (Rodríguez *et al.*, 2011), although these metals may also be present in Saharan dust (Galindo *et al.*, 2018; Quénel *et al.*, 2021). To provide insights into this issue, enrichment factors for V and Ni were calculated using Ti as the reference element (Rai *et al.*, 2021; Galindo *et al.*, 2017). The values obtained for both vanadium (EF_V = 3 in Elche and EF_V = 5 in Aitana) and nickel (EF_{Ni} = 9 in Elche and EF_{Ni} = 8 in Aitana) point to a predominantly crustal origin. Despite this, a certain contribution from shipping emissions to this factor cannot be ruled out, particularly in summer, when the predominant wind direction is from the sea (Clemente *et al.*, 2021).

e) *Aged sea salt*: the average mass concentration of this factor was not statistically different between both sites (2.9 µg m⁻³ in Elche and 2.7 µg m⁻³ in Aitana), although its relative contribution to PM_{10} at the mountain station was more than twice that found in Elche. At both locations this factor was characterized by high contributions from the typical marine ions Na^+ (42% of Na^+ mass in Elche and 63% in Aitana) and Mg^{2+} (30% and 48%, respectively), as well as SO_4^{2-} (72% and 39%, respectively) and $C_2O_4^{2-}$ (79% and 57%, respectively). At the Aitana station, the *Aged sea salt* factor explained the largest fraction of the mentioned species, while at the urban site this source was the major contributor to sulfate and oxalate. In this factor, Cl^- levels were very low as a result of the well-known reactions between airborne sea salt particles and atmospheric acidic species such as H_2SO_4 and HNO_3. These reactions lead to a deficit of Cl^- with respect to Na^+.

The *Aged sea salt* factor profile at the regional background station included a significant contribution of NO_3^- (33% of total NO_3^- was found in this source, only behind the *Nitrate* factor), while at the urban site nitrate was not present in this factor. This points to the presence of sodium nitrate in the aged marine source at Mt. Aitana. The absence of nitrate in this factor at the traffic site indicates that nitric acid reacts preferentially with calcium-rich particles to form $Ca(NO_3)_2$.

f) *Ammonium sulfate*: the concentration of the *Ammonium sulfate* factor was approximately the same at both locations (2.5 µg m⁻³ in Elche and 2.4 µg m⁻³ in Aitana).

This factor was characterized by high loadings of ammonium (87% of NH_4^+ was associated with this factor in Elche and 85% in Aitana) and sulfate (22% and 37% of SO_4^{2-}, respectively, was found in this factor) and is due to the regional background contribution of secondary ammonium sulfate.

g) *Fresh sea salt*: this factor represents sea spray aerosols that have not aged. As confirmed by the HYSPLIT model, the *Fresh sea salt* factor is associated with Atlantic advection episodes

This factor showed an average concentration of 1.8 µg m⁻³ in Elche (5% of PM_{10}) and 0.2 µg m⁻³ in Aitana (1% of PM_{10}). This difference was statistically significant and can be explained considering that in winter the mountain top is often decoupled from the PBL.

This factor explained the largest fraction of the total chloride mass (84% of Cl^- in Elche and 93% in Aitana) and was also characterized by high contributions from sodium (49% and 27% of Na^+, respectively, was explained by this factor) and magnesium (30% and 14% of Mg^{2+}, respectively, was found in this source). At both sites, the Mg^{2+}/Na^+ ratio was the same as that reported for sea water (0.12; Henderson and Henderson, 2009).

3.2.1 Seasonal variation of source contributions

a) Mt. Aitana

In wintertime (Fig. 4(a)) the *Nitrate* factor was the main contributor to PM_{10} due to the low impact from other sources. In contrast, during summer the Saharan dust source accounted for the largest fraction of the PM_{10} mass concentration, followed by the *Aged sea salt* and *Ammonium sulfate* factors. Marginal contributions from *Road traffic* and *Fresh sea-salt* were observed in both seasons.

The *Saharan dust* factor was the main contributor to PM_{10} in summer. The significant difference between the contribution from this factor in winter (22% of PM_{10}; 1.9 µg m⁻³) and summer months (37% of PM_{10}; 5.6 µg m⁻³) was due to the variability in the frequency and intensity of SDEs during
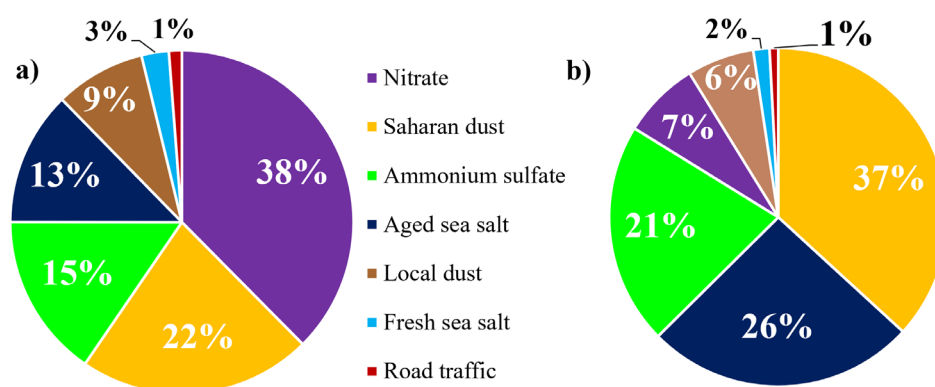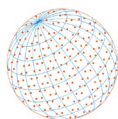
Fig. 4. Average contribution of PMF factors to PM$_{10}$ at the regional background station in (a) February and (b) July.

both seasons. It is well known that the occurrence of these episodes in the southeast of the Iberian Peninsula is usually highest in summer (Huerta-Viso *et al.*, 2020; Querol *et al.*, 2019). In the present study, the daily maximum concentration of Saharan dust was reached on 5 July (31.2 µg m^{-3}; ~74% of the daily PM$_{10}$ concentration), during an intense North African episode occurring between 04/07/19–08/07/19 (Fig. S3(a)).

The average concentration of the *Ammonium sulfate* factor in summer (3.2 µg m^{-3}; 21% of PM$_{10}$) was more than twice that in winter (1.3 µg m^{-3}; 15% of PM$_{10}$) due to the higher formation rate of this compound with increased solar radiation and temperature, and also to the fact that in winter this station is frequently above the PBL (Nicolás *et al.*, 2018).

The *Aged sea salt* factor showed the usual seasonal pattern (Fig. S3(b)), with a notably larger contribution to PM$_{10}$ in summer than in winter (Fig. 4). The prevalence of sea breezes in summer and the higher availability of atmospheric acidic species to react with sea spray would explain this result.

Regarding the *Local dust* factor, although its relative contribution to PM$_{10}$ was lower in summer than in winter (6% vs. 9%), its average mass concentration was statistically higher in summer (1.0 µg m^{-3}) than in winter (0.7 µg m^{-3}). The primary reason for this seasonal pattern is that the lower rainfall rate in summer favours soil dust resuspension.

Finally, the *Fresh sea salt* factor did not show any clear seasonal trend (Fig. S1(f)) and accounted for a similar percentage of the PM$_{10}$ mass concentration during both months (6% in February and 5% in July). Despite the proximity of Mt. Aitana to the Mediterranean coast, the complex orography of the terrain and the recirculation of air masses along the Mediterranean coast (Millán *et al.*, 1997) probably prevent fresh sea salt particles from reaching the sampling station without reacting with other pollutants.

b) Elche city center

The *Road traffic* source was the main contributor to PM$_{10}$ levels at the urban site, although it accounted for a larger fraction in February (38%, 13.4 µg m^{-3}) than in July (22%, 7.2 µg m^{-3}) (Fig. 5). This clear seasonal difference (Fig. S4(a)) has been observed in other studies (Clemente *et al.*, 2021; Scerri *et al.*, 2018; Yubero *et al.*, 2010) and can be explained by the lower dispersion conditions in the cold season. In fact, the highest mass concentration of this factor was reached on 27 February (26.4 µg m^{-3}), during a stagnation episode. Another reason for the higher contribution from this source in winter is that it also includes biomass burning emissions, as already mentioned.

The *Nitrate* factor also showed a significantly higher contribution to PM$_{10}$ levels in February (26% of PM$_{10}$; 9.2 µg m^{-3}) than in July (18% of PM$_{10}$; 5.9 µg m^{-3}) (Fig. 5). This can be due not only to reduced dispersion conditions in winter but also to the seasonal cycle of NH$_4$NO$_3$. Ammonium nitrate concentrations tend to be significantly lower in summer months due to its low thermal stability (Nicolás *et al.*, 2009).

The contribution of the *Local dust* factor did not show a statistically significant difference between winter and summer: 5.1 µg m^{-3} in February (15% of PM$_{10}$) and 5.6 µg m^{-3} in July (18% of
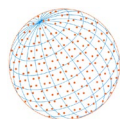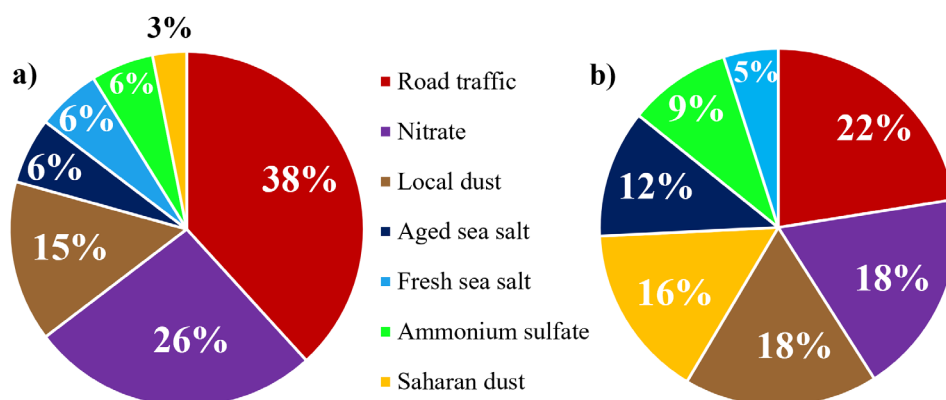
Fig. 5. Average contribution of PMF factors to PM_{10} at the urban background site in (a) February and (b) July of 2019.

PM_{10}). The lack of a clear seasonal trend for this factor could be due to the absence of rainfall in the city of Elche during the whole sampling period. Alternatively, atmospheric stagnation events typical of the winter season contribute to increase the concentrations of resuspended dust (Galindo *et al.*, 2020). For this reason, the highest contribution from this source to PM_{10} levels was registered on 27 February (Fig. S4(c)), the same as for the *Road traffic* factor.

The *Saharan dust* factor showed a similar temporal trend to that found in Aitana (Figs. S3(a) and S4(d)). The contribution from this factor was notably higher in summer (16% of PM_{10}; 5.0 µg m^{-3}) than in winter (3% of PM_{10}; 1.1 µg m^{-3}). The day with the highest concentration of African dust was 7 July (39.5 µg m^{-3}; ~70% of the daily PM_{10} concentration).

It must be noted that, during the study period, the impact of SDEs on PM_{10} levels is not always observed simultaneously at both sites. Moreover, the contribution of this factor to PM_{10} mass concentrations is usually higher at Mt. Aitana, probably due to high-altitude dust transport.

Regarding the *Aged sea salt* and *Ammonium sulfate* factors, both showed the same patterns as those observed at the mountain site, with higher contributions to PM_{10} levels in summer (12% and 9% of PM_{10}, respectively; 3.7 µg m^{-3} and 3.0 µg m^{-3}, respectively) than in winter (6% of PM_{10} each; ~2 µg m^{-3} each). Differences between the winter and summer values were statistically significant.

The average concentration of the *Fresh sea salt* factor was slightly higher in February (2.0 µg m^{-3}, 6% of the PM_{10} mass) than in July (1.6 µg m^{-3}, 5% of PM_{10} mass). This may be explained considering that this source is most likely related to the transport of marine aerosols during episodes of Atlantic advection and not to sea breezes coming from the Mediterranean. Additionally, the conversion of NaCl to Na_2SO_4 by the reaction between fresh sea salt and sulfuric acid is favoured in summer, as previously indicated.

4 CONCLUSIONS

The aim of this work was to identify PM_{10} sources having a regional reach and a local impact in the western Mediterranean basin. For that purpose, simultaneous sampling was carried out at a high-altitude mountain station and an urban traffic site during February and July of 2019. Seven sources with similar chemical profiles were identified at both sampling sites using the PMF model.

The main sources contributing to PM_{10} levels at the mountain site, named *Saharan dust*, *Aged sea salt* and *Ammonium sulfate*, had a regional influence since their mass concentrations were similar at both locations. Saharan dust levels were somewhat higher at the mountain station, probably because mineral dust particles are transported at high altitude. The *Road traffic* factor was associated with local vehicle exhaust and non-exhaust emissions at the urban station, being the major contributor to PM_{10} at this site (31% of the average PM_{10} mass). At the mountain site the contribution from this source to the measured PM_{10} concentration was marginal. Other factors such as *Nitrate* and *Local dust* showed little regional influence as they were significantly
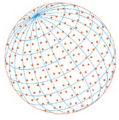
enhanced at the urban site. Atmospheric nitrate arises from the photochemical oxidation of NO_x emitted by road traffic, while a fraction of the local dust is derived from vehicle resuspension.

Seasonal differences in the concentrations of the identified sources were mainly explained by meteorology and the PBL height, as well as by the frequency and intensity of Saharan dust events (SDEs). These factors are crucial for the interpretation of the results at the high-altitude station, which under certain meteorological conditions can reside in the free troposphere.

At the urban site, local sources (*Road traffic*, *Nitrate* and *Local dust*) contributed ~80% to PM_{10} levels in winter. These results suggest that, at least in the cold season, mitigation strategies to reduce PM levels in non-industrialized urban areas should be focused on traffic emissions rather than on regional sources, which are more difficult to control.

ACKNOWLEDGEMENTS

ADDITIONAL INFORMATION AND DECLARATIONS

Author Contribution

Álvaro Clemente: Formal analysis, Investigation, Visualization, Writing-original draft, Writing-review and editing. Jose F. Nicolás: Writing-review and editing. Javier Crespo: Writing-review and editing. Carlos Pastor: Writing-review and editing. Nuria Galindo: Conceptualization, Writing-original draft, Supervision, Funding acquisition, Project administration. Eduardo Yubero: Conceptualization, Supervision, Formal analysis, Writing-review and editing, Funding acquisition, Project administration.

Funding

Data Availability

The data that support the findings of this study are available from the corresponding author upon reasonable request.

Ethics Approval

Not applicable.

Consent to Participate

Informed consent was obtained from all individual participants included in the study.
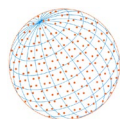
Consent for Publication

Consent to publish has been received from all participants.

### Competing Interests

The authors declare no competing interests.

Supplementary Material

Supplementary material for this article can be found in the online version at https://doi.org/10.4209/aaqr.230218
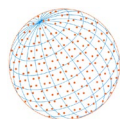
REFERENCES

Alebić-Juretić, A., Mifka, B. (2022). Sources of airborne particulates (PM_{10}) in the port city of Rijeka, Croatia. Environ. Sci. Pollut. Res. 29, 6578–6590. https://doi.org/10.1016/j.marpolbul.2021.112236

Baumann-Stanzer, K., Greilinger, M., Kasper-Giebl, A., Flandorfer, C., Hieden, A., Lotteraner, C., Ortner, M., Vergeiner, G., Schauer, G., Piringer, M. (2019). Evaluation of WRF-Chem model forecasts of a prolonged Saharan dust episode over the Eastern Alps. Aerosol Air Qual. Res. 19, 1226–1240. https://doi.org/10.4209/aaqr.2018.03.0116

Belis, C.A., Karagulian, F., Larsen, B.R., Hopke, P.K. (2013). Critical review and meta-analysis of ambient particulate matter source apportionment using receptor models in Europe. Atmos. Environ. 69, 94–108. https://doi.org/10.1016/j.atmosenv.2012.11.009

Bonvalot, L., Tuna, T., Fagault, Y., Sylvestre, A., Mesbah, B., Wortham, H., Jaffrezo, J.L., Marchand, N., Bard, E. (2019). Source apportionment of carbonaceous aerosols in the vicinity of a Mediterranean industrial harbor: A coupled approach based on radiocarbon and molecular tracers. Atmos. Environ. 2012, 250–261. https://doi.org/10.1016/j.atmosenv.2019.04.008

Borlaza, L.J., Weber, S., Marsal, A., Uzu, G., Jacob, V., Besomes, J.L., Chatain, M., Conil, S., Jafrezzo, J.L. (2022). Nine-year trends of PM_{10} sources and oxidative potential in a rural background site in France. Atmos. Chem. Phys. 22, 8701–8723. https://doi.org/10.5194/acp-22-8701-2022

Castañer, R., Nicolás, J.F., Crespo, J., Yubero, E., Galindo, N., Caballero, S., Pastor, C. (2017). Influence of air mass origins on optical properties and PM concentrations measured at high mountain stations located in the southwestern Mediterranean. Atmos. Res. 197, 244–254. https://doi.org/10.1016/j.atmosres.2017.07.013

Cavalli, F., Viana, M., Yttri, K.E., Genberg, J., Putaud, J.P. (2010). Toward a standardized thermal-optical protocol for measuring atmospheric organic and elemental carbon: the EUSAAR protocol. Atmos. Meas. Tech. 3, 79–89. https://doi.org/10.5194/amt-3-79-2010

Cerro, J.C., Cerdá, V., Querol, X., Alastuey, A., Pey, J. (2020). Variability of air pollutants, and PM composition and sources at a regional background site in the Balearic Islands: Review of western Mediterranean phenomenology from a 3-year study. Sci. Total Environ. 717, 137177. https://doi.org/10.1016/j.scitotenv.2020.137177

Cesari, D., De Benedetto, G.E., Bonasoni, P., Busetto, M., Dinoi, A., Merico, E., Chirizzi, D., Cristofanelli, P., Donateo, A., Grasso, F.M., Marinoni, A., Pennetta, A., Contini, D. (2018). Seasonal variability of $PM_{2.5}$ and PM_{10} composition and sources in an urban background site in Southern Italy. Sci. Total Environ. 612, 202–213. https://doi.org/10.1016/j.scitotenv.2017.08.230

Chiari, M., Yubero, E., Calzolai, G., Lucarelli, F., Crespo, J., Galindo, N., Nicolás, J.F., Giannoni, M., Nava, S. (2018). Comparison of PIXE and XRF analysis of airborne particulate matter samples collected on Teflon and quartz fibre filters. Nucl. Instrum. Methods Phys. Res. 417, 128–132. https://doi.org/10.1016/j.nimb.2017.07.031

Clemente, Á., Yubero, E., Galindo, N., Crespo, J., Nicolás, J.F., Santacatalina, M., Carratala, A. (2021). Quantification of the impact of port activities on PM_{10} levels at the port-city boundary of a Mediterranean city. J. Environ. Manage. 281, 111842. https://doi.org/10.1016/j.jenvman.2020.111842

Corbin, J.C., Mensah, A.A., Pieber, S.M., Orasche, J., Michalke, B., Zanatta, M., Czech, H., Massabò, D., Buatier de Mongeot, F., Mennucci, C., El Haddad, I., Kumar, N.K., Stengel, B., Huang, Y., Zimmermann, R., Prévôt, A.S.H., Gysel, M. (2018). Trace metals in soot and $PM_{2.5}$ from heavy-fuel-oil combustion in a marine engine. Environ. Sci. Technol. 52, 6714–6722. https://doi.org/10.1021/acs.est.8b01764

Cristofanelli, P., Brattich, E., Decesari, S., Landi, T.C., Maione, M., Putero, D., Tositti, L., Bonasoni, P. (2018). High-mountain atmospheric research. The Italian Mt. Cimone WMO/GAW global station 2165 m a.s.l. Springer Briefs in Meteorology.

Daellenbach, K.R., Uzu, G., Jiang, J., Cassagnes, L.E., Leni, Z., Vlachou, A., Stefanelli, G., Canonaco, F., Weber, S., Segers, A., Kuenen, J.J.P., Schaap, M., Favez, O., Albinet, A., Aksoyoglu, S., Dommen, J., Baltensperger, U., Geiser, M., El Haddad, I., Jaffrezo, J.L., Prévôt, A.S.H. (2020). Sources of
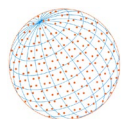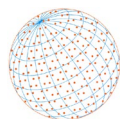
particulate-matter air pollution and its oxidative potential in Europe. Nature 587, 414–419. https://doi.org/10.1038/s41586-020-2902-8

Dawson, M.L., Varner, M.E., Perraud, V., Ezell, M.J., Gerber, R.B., Finlayson-Pitts, B.J. (2012). Simplified mechanism for new particle formation from methanesulfonic acid, amines, and water via experiments and ab initio calculations. Proc. Natl. Acad. Sci. U.S.A. 109, 18719–18724. https://doi.org/10.1073/pnas.1211878109

Deabji, N., Fomba, K.W., El Hajjaji, S., Mellouki, A., Poulain, L., Zeppenfeld, S., Herrmann, H. (2021). First insights into northern Africa high-altitude background aerosol chemical composition and source influences. Atmos. Chem. Phys. 21, 18147–18174. https://doi.org/10.5194/acp-21-18147-2021

Decesari, S., Facchini, M. C., Carbone, C., Giulianelli, L., Rinaldi, M., Finessi, E., Fuzzi, S., Marinoni, A., Cristofanelli, P., Duchi, R., Bonasoni, P., Vuillermoz, E., Cozic, J., Jaffrezo, J.L., Laj, P. (2010). Chemical composition of PM_{10} and PM_1 at the high-altitude Himalayan station Nepal Climate Observatory-Pyramid (NCO-P) (5079 m a.s.l.). Atmos. Chem. Phys. 10, 4583–4596. https://doi.org/10.5194/acp-10-4583-2010

Diapouli, E., Manousakas, M.I., Vratolis, S., Vasilatou, V., Pateraki, S., Bairachtari, K.A., Querol, X., Amato, F., Alastuey, A., Karanasiou, A.A., Lucarelli, F., Nava, S., Calzolai, G., Gianelle, V.L., Colombi, C., Alves, C., Custódio, D., Pio, C., Spyrou, C., Kallos, G.B., et al. (2017). AIRUSE-LIFE +: estimation of natural source contributions to urban ambient air $PM_{2.5}$ concentrations in southern Europe – implications to compliance with limit values. Atmos. Chem. Phys. 17, 3673–3685. https://doi.org/10.5194/acp-17-3673-2017

Dimitriou, K., Grivas, G., Liakakou, E., Gerasopoulos, E., Mihalopoulos, N. (2021). Assessing the contribution of regional sources to urban air pollution by applying 3D-PSCF modeling. Atmos. Res. 248, 105187. https://doi.org/10.1016/j.atmosres.2020.105187

Dimitriou, K., Kassomenos, P. (2017). Aerosol contributions at an urban background site in Eastern Mediterranean – Potential source regions of PAHs in PM_{10} mass. Sci. Total Environ. 598, :563–571. https://doi.org/10.1016/j.scitotenv.2017.04.164

Ealo, M., Alastuey, A., Pérez, N., Ripoll, A., Querol, X., Pandolfi, M. (2018). Impact of aerosol particle sources on optical properties in urban, regional and remote areas in the north-western Mediterranean. Atmos. Chem. Phys. 18, 1149–1169. https://doi.org/10.5194/acp-18-1149-2018

European Environment Agency (EEA) (2012). Particulate matter from natural sources and related reporting under the EU Air Quality Directive in 2008 and 2009. EEA Technical report No 10/2012. Publications Office of the European Union, Luxembourg. https://www.eea.europa.eu/publications/particulate-matter-from-natural-sources/at_download/file

Furman, P., Styszko, K., Skiba, A., Zięba, D., Zimnoch, M., Kistler, M., Kasper-Giebl, A., Gilardoni, S. (2021). Seasonal variability of PM_{10} chemical composition including 1,3,5-triphenylbenzene, marker of plastic combustion and toxicity in Wadowice, South Poland. Aerosol Air Qual. Res. 21, 200223. https://doi.org/10.4209/aaqr.2020.05.0223

Galindo, N., Yubero, E., Nicolás, J.F., Crespo, J., Soler, R. (2016). Chemical characterization of PM_1 at a regional background site in the western Mediterranean. Aerosol Air Qual. Res. 16, 530–541. https://10.4209/aaqr.2015.05.0302

Galindo, N., Yubero, E. (2017). Day-night variability of water-soluble ions in PM_{10} samples collected at a traffic site in southeastern Spain. Environ. Sci. Pollut. Res. 24, 805–812. https://doi.org/10.1007/s11356-016-7836-1

Galindo, N., Yubero, E., Nicolás, J.F., Crespo, J., Varea, M., Gil-Moltó, J. (2017). Regional and long-range transport of aerosols at Mt. Aitana, Southeastern Spain. Sci. Total Environ. 584–585, 723–730. https://10.1016/j.scitotenv.2017.01.108

Galindo, N., Yubero, E., Nicolás, J.F., Varea, M., Crespo, J. (2018). Characterization of metals in PM_1 and PM_{10} and health risk evaluation at an urban site in the western Mediterranean. Chemosphere 201, 243–250. https://doi.org/10.1016/j.chemosphere.2018.02.162

Galindo, N., Yubero, E., Clemente, A., Nicolás, J.F., Navarro-Selma, B., Crespo, J. (2019). Insights into the origin and evolution of carbonaceous aerosols in a Mediterranean urban environment. Chemosphere 235, 636–642. https://doi.org/10.1016/j.chemosphere.2019.06.202

Galindo, N., Yubero, E., Clemente, A., Nicolás, J.F., Varea, M., Crespo, J. (2020). PM events and
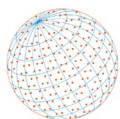
changes in the chemical composition of urban aerosols: A case study in the western Mediterranean. Chemosphere 244, 125520. https://doi.org/10.1016/j.chemosphere.2019.125520

Galindo, N., Clemente, Á., Yubero, E., Nicolás, J.F., Crespo, J. (2021). PM_{10} chemical composition at a residential site in the western Mediterranean: Estimation of the contribution of biomass burning from levoglucosan and its isomers. Environ. Res. 196, 110394. https://doi.org/10.1016/j.envres.2020.110394

Grantz, D.A., Garner, J.H.B., Johnson, D.W. (2003). Ecological effects of particulate matter. Environ. Int. 29, 213–239. https://doi.org/10.1016/S0160-4120(02)00181-2

Groma, V., Aföldi, B., Börcsök, E., Czömpöly, O., Füri, P., Kéri, A.H., Kovács, G., Török, S., Osán, J. (2022). Sources and health effects of fine and ultrafine aerosol particles in an urban environment. Atmos. Pollut. Res. 13, 101302. https://doi.org/10.1016/j.apr.2021.101302

Hama, S.M.L., Cordell, R.L., Staelens, J., Mooibroek, D., Monks, P.S. (2018). Chemical composition and source identification of PM_{10} in five North Western European cities. Atmos. Res. 214, 135–149. https://doi.org/10.1016/j.atmosres.2018.07.014

Harrison, R.M., Allan, J., Carruthers, D., Heal, M.R., Lewis, A.C., Marner, B., Murrells, T., Williams, A. (2021). Non-exhaust vehicle emissions of particulate matter and VOC from road traffic: A review. Atmos. Environ. 262, 118592. https://doi.org/10.1016/j.atmosenv.2021.118592

Henderson, P., Henderson, G.M. (2009). The Cambridge Handbook of Earth science data. Cambridge University Press, pp. 92–97.

Hopke, P.K., Croft, D., Zhang, W., Lin, S., Masiol, M., Squizzato, S., Thurston, S.W., van Wijngaarden, E., Utell, M.J., Rich, D.Q. (2020a). Changes in the hospitalizations and emergency department visits for respiratory diseases to source-specific $PM_{2.5}$ in New York state from 2005 to 2016. Environ. Res. 181, 108912. https://10.1016/j.envres.2019.108912

Hopke, P.K., Dai, Q., Li, L., Feng, Y. (2020b). Global review of recent source apportionments for airborne particulate matter. Sci. Total Environ. 740, 140091. https://doi.org/10.1016/j.scitotenv.2020.140091

Huerta-Viso, A., Crespo, J., Galindo, N., Yubero, E., Nicolás, J.F. (2020). Saharan dust events over the Valencian Community (Eastern Iberian Peninsula): Synoptic circulation patterns and contribution to PM_{10} levels. Aerosol Air Qual. Res. 20, 2519–2528. https://doi.org/10.4209/aaqr.2020.01.0038

Jain, S., Sharma, S.K., Vijayan, N., Mandal, T.K. (2020). Seasonal characteristics of aerosols ($PM_{2.5}$ and PM_{10}) and their source apportionment using PMF: A four year study over Delhi, India. Environ. Pollut. 262, 114337. https://doi.org/10.1016/j.envpol.2020.114337

Ji, H., Shao, M., Wang, Q. (2020). Contribution of meteorological conditions to inter-annual variations in air quality during the past decade in Eastern China. Aerosol Air Qual. Res. 20, 249–2259. https://doi.org/10.4209/aaqr.2019.12.0624

Keuken, M.P., Zandveld, P., Jonkers, S., Moerman, M., Jedynska, A.D., Verbeek, R., Visschedijk, A., Elshout van den, S., Panteliadis, P., Velders, G.J.M. (2013). Modelling elemental carbon at regional, urban and traffic locations in The Netherlands. Atmos. Environ. 73, 73–80. https://doi.org/10.1016/j.atmosenv.2013.03.010

Khanna, I., Khare, M., Gargava, P., Khan, A.A. (2018). Effect of $PM_{2.5}$ chemical constituents on atmospheric visibility impairment. J. Air Waste Manage. Assoc. 68, 430–437. https://10.1080/10962247.2018.1425772

Kim, K.Y., Kabir, E., Kabir, S. (2015). A review on the human health impact of airborne particulate matter. Environ. Int. 74, 136–143. https://10.1016/j.envint.2014.10.005

Marenco, F., Bonasoni, P., Ceriani, M., Cristofanelli, P., D'Alessandro, A., Fermo, P., Lucarelli, F., Mazzei, F., Nava, S., Piazzalunga, A., Prati, P., Valli, G., Vecchi, R. (2006). Characterization of atmospheric aerosols at Monte Cimone, Italy, during summer 2004: Source apportionment and transport mechanisms. J. Geophys. Res. 111, D24202. https://doi.org/10.1029/2006JD007145

Megido, L., Negral, L., Castrillón, L., Marañón, E., Fernández-Nava, Suárez-Peña, B. (2016). Traffic tracers in a suburban location in northern Spain: relationship between carbonaceous fraction and metals. Environ. Sci. Pollut. Res. 23, 8669–8678. https://10.1007/s11356-015-5955-8

Millán, M.M., Salvador, R., Mantilla, E., Kallos, G. (1997). Photooxidant dynamics in the Mediterranean basin in summer: Results from European research projects. J. Geophys. Res. 102, 8811–8823. https://doi.org/10.1029/96JD03610

Millán-Martínez, M., Sánchez-Rodas, D., Sánchez de la Campa, A.M., de la Rosa, J. (2021). Contribution of anthropogenic and natural sources in PM$_{10}$ during North African dust events in Southern Europe. Environ. Pollut. 290, 118065. https://doi.org/10.1016/j.envpol.2021.118065

Moroni, B., Castellini, S., Crocchianti, S., Piazzalunga, A., Fermo, P., Scardazza, F., Cappelletti, D. (2015). Ground-based measurements of long-range transported aerosol at the rural regional background site of Monte Martano (Central Italy). Atmos. Res. 155, 26–36. https://doi.org/10.1016/j.atmosres.2014.11.021

Nault, B.A., Jo, D.S., McDonald, B.C., Campuzano-Jost, P., Day, D.A., Hu, W., Schroder, J.C., Allan, J., Blake, D.R., Canagaratna, M.R., Coe, H., Coggon, M.M., DeCarlo, P.F., Diskin, G.S., Dunmore, R., Flocke, F., Fried, A., Gilman, J.B., Gkatzelis, G., Hamilton, J.F., et al. (2021). Secondary organic aerosols from anthropogenic volatile organic compounds contribute substantially to air pollution mortality. Atmos. Chem. Phys. 21, 11201–11224. https://doi.org/10.5194/acp-21-11201-2021

Navarro-Selma, B., Clemente, A., Nicolás, J.F., Crespo, C., Carratalá, A., Lucarelli, F., Giardi, F., Galindo, N., Yubero, E. (2022). Size segregated ionic species collected in a harbour area. Chemosphere 294, 133693. https://doi.org/10.1016/j.chemosphere.2022.133693

Nicolás, J.F., Chiari, M., Crespo, J., Garcia Orellana, I., Lucarelli, F., Nava, S., Pastor, C., Yubero, E. (2008). Quantification of Saharan and local dust impact in an arid Mediterranean area by the positive matrix factorization (PMF) technique. Atmos. Environ. 42, 8872–8882. https://doi.org/10.1016/j.atmosenv.2008.09.018

Nicolás, J.F., Galindo, N., Yubero, E., Pastor, C., Esclapez, R., Crespo, J. (2009). Aerosol inorganic ions in a semiarid region on the southeastern Spanish Mediterranean Coast. Water Air Soil Pollut. 201, 49–159. https://doi.org/10.1007/s11270-008-9934-2

Nicolás, J.F., Castañer, R., Crespo, J., Yubero, E., Galindo, N., Pastor, C. (2018). Seasonal variability of aerosol absorption parameters at a remote site with high mineral dust loads. Atmos. Res. 210, 100–109. https://doi.org/10.1016/j.atmosres.2018.04.008

Paatero, P., Tapper, U. (1994). Positive matrix factorization: A non-negative factor model with optimal utilization of error estimates of data values. Environmetrics 5, 111–126. https://doi.org/10.1002/env.3170050203

Paatero, P., Hopke, P.K. (2003). Discarding or downweighting high-noise variables in factor analytic models. Anal. Chim. Acta. 490, 277–289. https://doi.org/10.1016/S0003-2670(02)01643-4

Pandolfi, M., Mooibroek, D., Hopke, P., Van Pinxteren, D., Querol, X., Herrmann, H., Alastuey, A., Favez, O., Hüglin, C., Perdrix, E., Riffault, V., Sauvage, S., Van Der Swaluw, E., Tarasova, O., Colette, A. (2020). Long-range and local air pollution: what can we learn from chemical speciation of particulate matter at paired sites? Atmos. Chem. Phys. 20, 409–429. https://doi.org/10.5194/acp-20-409-2020

Piscitello, A., Bianco, C., Casasso, A., Sethi, R. (2021). Non-exhaust traffic emissions: Sources, characterization, and mitigation measures. Sci. Total Environ. 766, 144440. https://doi.org/10.1016/j.scitotenv.2020.144440

Priyan, R.S., Peter, A.E., Menon, J.S., George, M., Shiva Nagendra, S.M., Khare, M. (2022). Composition, sources, and health risk assessment of particulate matter at two different elevations in Delhi city. Atmos. Pollut. Res. 13, 10129. https://doi.org/10.1016/j.apr.2021.101295

Quénel, P., Vadel, J., Garbin, C., Durnad, S., Favez, O., Albinet, A., Raghoumandan, C., Guyomard, S., Alleman, L.Y., Mercier, F. (2021). PM$_{10}$ chemical profile during North African dust episodes over French West Indies. Atmosphere 12, 277. https://doi.org/10.3390/atmos12020277

Querol, X., Pérez, N., Reche, C., Ealo, M., Ripoll, A., Tur, J., Pandolfi, M., Pey, J., Salvador, P., Moreno, T., Alastuey, A. (2019). African dust and air quality over Spain: Is it only dust that matters? Sci. Total Environ. 686, 737–752. https://doi.org/10.1016/j.scitotenv.2019.05.349

Rai, P., Slowik, J.G., Furger, M., El Haddad, I., Visser, S., Tong, Y., Singh, A., Wehrle, G., Kumar, V., Tobler, A.K., Bhattu, D., Wang, L., Ganguly, D., Rastogi, N., Huang, R.J., Necki, J., Cao, J., Tripathi, S.N., Baltensperger, U., Prévôt, A.S.H. (2021). Highly time-resolved measurements of element concentrations in PM$_{10}$ and PM$_{2.5}$ comparison of Delhi, Beijing, London, and Krakow. Atmos. Chem. Phys. 21, 717–730. https://doi.org/10.5194/acp-21-717-2021

Ram, K., Sarim, M.M., Hedge, P. (2010). Long-term record of aerosol optical properties and chemical composition from a high-altitude site (Manora Peak) in Central Himalaya. Atmos. Chem. Phys. 10, 11791–11803. https://doi.org/10.5194/acp-10-11791-2010

Ramírez, O., Sánchez de la Campa, A.M., Amato, F., Catacolí, R.A, Rojas, N.Y., de la Rosa, J. (2018). Chemical composition and source apportionment of PM$_{10}$ at an urban background site in a high altitude Latin American megacity (Bogota, Colombia). Environ. Pollut. 233, 142–155. https://doi.org/10.1016/j.envpol.2017.10.045

Ripoll, A., Minguillón, M.C., Pey, J., Pérez, N., Querol, X., Alastuey, A. (2015). Joint analysis of continental and regional background environments in the western Mediterranean: PM$_1$ and PM$_{10}$ concentrations and composition. Atmos. Chem. Phys. 15, 1129–1145. https://doi.org/10.5194/acp-15-1129-2015

Rodríguez, S., Alastuey, A., Alonso-Pérez, S., Querol, X.; Cuevas, E., Abreu-Afonso, J., Viana, M., Pérez, N., Pandolfi, M., de la Rosa, J. (2011). Transport of desert dust mixed with North African industrial pollutants in the subtropical Saharan Air Layer. Atmos. Chem. Phys. 11, 6663–6685. https://doi.org/10.5194/acp-11-6663-2011

Salvador, P., Artíñano, B., Pio, C., Afonso, J., Legrand, M., Puxbaum, H., Hammer, S. (2010). Evaluation of aerosol sources at European high altitude background sites with trajectory statistical methods. Atmos. Environ. 44, 2316–2329. https://doi.org/10.1016/j.atmosenv.2010.03.042

Samek, L., Styszko, K., Stegowski, Z., Zimnoch, M., Skiba, A., Turek-Fijak, A., Gorczyca, Z., Furman, P., Kasper-Giebl, A., Rozanski, K. (2021). Comparison of PM$_{10}$ sources at traffic and urban background sites based on elemental, chemical and isotopic composition: case study from Krakow, Southern Poland. Atmosphere 12, 1364. https://doi.org/10.3390/atmos12101364

Scerri, M.M., Kandler, K., Weinbruch, S., Yubero, E., Galindo, N., Prati, P., Caponi, L., Massabò, D. (2018). Estimation of the contributions of the sources driving PM$_{2.5}$ levels in a Central Mediterranean coastal town. Chemosphere 211, 465–481. https://doi.org/10.1016/j.chemosphere.2018.07.104

Tsamalis, C., Ravetta, F., Gheusi, F., Delbarre, H., Augustin, P. (2014). Mixing of free-tropospheric air with the lowland boundary layer during anabatic transport to a high altitude station. Atmos. Res. 143, 425–437. https://doi.org/10.1016/j.atmosres.2014.03.011

Valenzuela, A., Olmo, F.J., Lyamany, H., Antón, M., Titos, G., Cazorla, A., Alados-Arboledas, L. (2015). Aerosol scattering and absorption Angström exponents as indicators of dust and dust-free days over Granada (Spain). Atmos. Res. 154, 1–13. https://doi.org/10.1016/j.atmosres.2014.10.015

van Drooge, B.L., Garatachea, R., Reche, C., Titos, G., Alastuey, A., Lyamani, H., Alados-Arboledas, L., Querol, X., Gimalt, J.O. (2022). Primary and secondary organic winter aerosols in Mediterranean cities under different mixing layer conditions (Barcelona and Granada). Environ. Sci. Pollut. Res. 29, 36255–36272. https://doi.org/10.1007/s11356-021-16366-0

Viana, M., Pey, J., Querol, X., Alastuey, A., de Leeuw, F., Lükewille, A. (2014). Natural sources of atmospheric aerosols influencing air quality across Europe. Sci. Total Environ. 472, 825–833. https://doi.org/10.1016/j.scitotenv.2013.11.140

Wang, W., Maenhaut, W., Yang, W., Liu, X., Bai, Z., Zhang, T., Claeys, M., Cachier, H., Dong, S., Wang, Y. (2014). One–year aerosol characterization study for PM$_{2.5}$ and PM$_{10}$ in Beijing. Atmos. Pollut. Res. 5, 554–562. https://doi.org/10.5094/APR.2014.064

Weber, S., Salameh, D., Albinet, A., Alleman, L.Y., Waked, A., Besombes, J.L., Jacob, V., Guillaud, G., Meshbah, B., Rocq, B., Hulin, A., Dominik-Sègue, M., Chrétien, E., Jaffrezo, J.L., Favez, O. (2019). Comparison of PM$_{10}$ source profiles at 15 French sites using a harmonized constrained positive matrix factorization approach. Atmosphere 10, 310. https://doi.org/10.3390/atmos10060310

Wei, J., Hou, T., Li, Z., Guo, S., Li, Z. (2022). Changes in chemical composition, sources, and health risk of PM$_{2.5}$ with sand storm at a small city in North China. Aerosol Air Qual. Res. 22, 220114. https://doi.org/10.4209/aaqr.220114

Yubero, E., Carratalá, A., Crespo, J., Nicolás, J., Santacatalina, M., Nava, S., Lucarelli, F., Chiari, M. (2010). PM$_{10}$ source apportionment in the surroundings of the San Vicente del Raspeig cement plant complex in southeastern Spain. Environ. Sci. Pollut. Res. 18, 64–74. https://doi.org/10.1007/s11356-010-0352-9

Zhang, R.J., Ho, K.F., Shen, Z.X. (2012). The role of aerosol in climate change, the environment, and human health. Atmos. Ocean Sci. Lett. 5, 156–161. https://doi.org/10.1080/16742834.2012.11446983

Zhang, X., Murakami, T., Wang, J., Aikawa, M. (2021). Sources, species and secondary formation
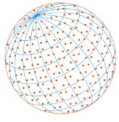
of atmospheric aerosols and gaseous precursors in the suburb of Kitakyushu, Japan. Sci. Total Environ. 763, 143001. https://doi.org/10.1016/j.scitotenv.2020.143001